NATIONAL ADVISORY COMMITTEE FOR AERONAUTICS

WARTIME REPORT

ORIGINALLY ISSUED

June 1945 as
Advance Confidential Report E5E19

THE EFFECT OF INLET PRESSURE AND TEMPERATURE ON THE

EFFICIENCY OF A SINGLE-STAGE IMPULSE TURBINE HAVING

AN 11.0-INCH PITCH-LINE DIAMETER WHEEL

By David S. Gabriel, L. Robert Carman
and Elmer E. Trautwein

Aircraft Engine Research Laboratory
Cleveland, Ohio

NACA

WASHINGTON

NACA ACR No. E5E19

THE EFFECT OF INLET PRESSURE AND TEMPERATURE ON THE EFFICIENCY

OF A SINGLE-STAGE IMPULSE TURBINE HAVING AN

11.0-INCH PITCH-LINE DIAMETER WHEEL

By David S. Gabriel, L. Robert Carman
and Elmer E. Trautwein

SUMMARY

Efficiency tests have been conducted on a single-stage impulse turbine having an 11.0-inch pitch-line diameter wheel with inserted buckets and a fabricated nozzle diaphragm. The tests were made to determine the effect of inlet pressure, inlet temperature, speed, and pressure ratio on the turbine efficiency. An analysis is presented that relates the effect of inlet pressure and temperature to the Reynolds number of the flow. The agreement between the analysis and the experimental data indicates that the changes in turbine efficiency with inlet pressure and temperature may be principally a Reynolds number effect.

INTRODUCTION

The efficiency of turbines is conventionally represented as a function of the blade-to-jet speed ratio and the pressure ratio. Some data are available in the literature on the effect of these variables on turbine performance. It has been generally assumed that the effects on performance of inlet pressure and temperature for a given blade-to-jet speed ratio and pressure ratio are small. No data on these effects could be found.

Adequate test facilities are not always available for testing turbines under actual operating conditions and experimenters often test at the proper blade-to-jet speed ratios and pressure ratios but at inlet temperatures and pressures that differ from actual operating conditions. Because of the need for information on the effects of inlet temperature and pressure in addition to the effects of blade-to-jet speed ratio and pressure ratio, the NACA Cleveland laboratory conducted tests from July to October 1944 on an exhaust-gas turbine using both hot gases and air as the driving fluids. These tests cover a range of inlet pressures from 10 to 60 inches

of mercury absolute, inlet temperatures from 550° to 2000° F absolute, and pressure ratios from 1.4 to 5.2. A method of correlation of the data is presented in this report.

An attempt is also made to correlate the effects of inlet pressure and temperature by introducing the Reynolds number. An analysis that shows the relation of the inlet pressure and temperature to the Reynolds number is presented.

APPARATUS

A single-stage impulse turbine having an 11.0-inch pitch-line diameter wheel with inserted buckets and a fabricated nozzle diaphragm was tested. Bucket-to-nozzle clearance was set at 0.138 inch. A high-speed hydraulic dynamometer was coupled to the shaft to absorb the turbine power. The general arrangement of the experimental test setup and the piping system including the hot-gas producer is shown in figures 1 and 2.

The turbine was driven by air at 550° F absolute and hot gases at various inlet temperatures and pressures. An A.S.M.E. orifice installed in the combustion-air piping ahead of the hot-gas producer was used to measure the air flow. The gas temperature at the nozzle-box inlet was measured with a quadruple-shielded chromel-alumel thermocouple and a self-balancing potentiometer. This temperature was taken to be the total temperature at the nozzle-box inlet. The static pressure at the nozzle-box inlet was measured in a manifold connected to four pressure taps in the same cross section of the inlet pipe.

The driving fluid was discharged from the turbine into a plenum chamber, which was directly connected to an altitude-exhaust system. The static pressure in the plenum chamber was taken as the bucket discharge pressure p_d. The static-pressure tap for measuring the discharge pressure was located about 1/2 inch behind the external cooling cap, as shown by the detailed sketch in figure 3. The end of the pressure-tap tube was plugged and a hole was drilled about 1/4 inch from the end of the tube on the downstream side. All pressures were measured with mercury manometers. The location of the points where temperature and pressure measurements were made is shown in figure 3.

Leakage of air between the atmosphere and the turbine was prevented by a housing around the turbine-bearing assembly and by plugs welded into the openings in the annular support between the nozzle box and the nozzle-box baffle. A labyrinth seal gland was installed around the turbine shaft between the housing and a pressure-balancing

chamber, which could be evacuated by a jet pump or pressurized by compressed air. Leakage of air between the chamber and the housing was prevented by adjusting the pressure in the pressure-balancing chamber until a manometer connected to the two spaces between the rings of the labyrinth seal gland showed zero pressure drop. Cooling caps placed in close proximity to both sides of the turbine wheel and cooled by water provided some cooling of the wheel and the bearing housing.

Dynamometer-torque measurements were made with an NACA balanced-diaphragm torque indicator (reference 1). The turbine speed was measured with a standard engine tachometer. The tachometer was fitted with an enlarged indicating dial having very fine divisions to increase the accuracy and the ease of reading the instrument. Two tachometer generators were used to cover the range of turbine speeds in this test. One of the generators turned at the same speed as the turbine tachometer drive and the other turned at twice the speed. The higher-speed generator was used at the low turbine speeds for greater accuracy of speed measurement.

The nozzle box was insulated for the final series of tests. The insulation used was an asbestos base material, which was plastered directly on the nozzle box with a thickness from 1 to 2 inches.

A cross section of the hot-gas producer is shown in figure 4. Air passes through the orifice, enters the producer near the top, and flows downward through the annular space between the inner and the outer shells to provide cooling for the shells. The air is turned through an arc of 180° at the bottom of the producer, where the flow is divided between the space provided for the igniter-nozzle assemblies and the two vaned sections.

The producer has eight igniter-nozzle assemblies and can be operated with any number of the igniter-nozzle assemblies in use. Each igniter assembly has a fuel-spray nozzle with a double-electrode igniter, which furnishes continuous ignition. The fuel flow to the nozzles is individually controlled by needle valves in the lines to the fuel nozzles. The temperature of the gas is varied by using a different size or number of nozzles. Small adjustments of temperature are made by throttling the fuel lines to change the fuel pressure at the spray nozzles. The fuel flow is measured with a calibrated rotameter.

The air is heated by burning gasoline, which is injected through the fuel nozzles. No fuel was burned for the tests at 550° F absolute. The gases flow from the producer to the turbine nozzle box through a pipe approximately 23 feet long and insulated with a 3-inch thickness of mixed asbestos fiber and milled silica held in place by

a larger duct that encloses the pipe conveying the hot gases. A diagram of the inlet pipe is shown in figure 4. The pipe diameter changes from 10 to 6 inches before it is connected to the turbine nozzle box.

Before the turbine was installed, temperature and total-pressure surveys were made in the piping system at a point approximately 8 inches upstream from the flange to which the nozzle box was attached. Traverses were made across 2 diameters of the 6-inch pipe at right angles to each other. At a gas temperature of 1400° F, a variation of 10° F was found. Total-pressure surveys were made at different gas temperatures for a weight flow of approximately 2.2 pounds per second. There was no variation in total pressure within a 5-inch-diameter circle with its center line on the center line of the 6-inch pipe. At points 1/4 inch from the pipe wall, the total pressure was found to be approximately 75 percent of the total pressure measured in the center of the pipe. These tests indicated that the velocity and the temperature profiles across the pipe were very uniform.

Although these surveys were made with impact tubes, the total pressure at the inlet to the turbine for the test data was computed by adding the measured static pressure at the nozzle-box inlet to the average velocity pressure computed from the continuity equation. The use of the continuity equation was justified by the existence of the flat velocity and temperature profiles.

The outside wheel diameter was measured at intervals throughout the tests. No measurable stretching of the wheel was observed at the end of the tests.

ACCURACY

The method suggested by the A.S.M.E. for estimating the accuracy of measurement of air flow utilizing their orifice data gives a probable error of ±1.17 percent. Turbine-shaft torque was measured to the nearest 0.15 foot-pound. The tachometers were calibrated and the readings taken in the tests were corrected by use of the calibration curve. The turbine-speed measurements were accurate to ±15 rpm for speeds from 0 to 17,000 rpm and ±30 rpm for speeds from 17,000 to 21,000 rpm. All pressure readings were taken to 0.05 inch of mercury.

TESTS

Efficiency tests were made over a range of inlet temperatures and pressures and pressure ratios. The following table shows the approximate test conditions:

Pressure ratio p_1/p_d	Total inlet pressure p_1 (in. Hg abs.)	Total inlet temperature T_1 (°F abs.)
Tests with uninsulated nozzle box; speed range, 3000 to 21,000 rpm		
1.4, 2.2, 3.0, 3.9, 5.2	27	550
		1200
		1800
1.4, 2.2, 3.0	10	1200
	19	
	27	
	35	
	43	
	52	
	60	
1.4, 2 2, 3.0	27	1600
		2000
Tests with uninsulated nozzle box; constant blade-to-jet speed ratio, 0.4		
2.2	52	1000
	35	2000
	19	1400
	19	1800
	10	1800
Tests with insulated nozzle box; speed range 3000 to 21,000 rpm		
1.4, 2.2, 3.0, 3.9, 5.2	27	1200
2.2	27	1000
		1600
		1800

SYMBOLS

A_d annular area swept by turbine buckets (sq ft)

g acceleration due to gravity, 32.2 (ft)/(sec)^2 or dimensional constant, 32.2 (lb)/(slug)

M_a mass flow of air (slugs)/(sec)

M_t mass flow of air plus fuel (slugs)/(sec)

N turbine speed (rpm)

p_d static pressure of turbine discharge at plenum chamber
          (in. Hg absolute)

p_1 total pressure at nozzle-box inlet (in. Hg absolute)

P_t turbine shaft power (ft-lb)/(sec)

P_{th} theoretical turbine power available for expansion from inlet
          total temperature and pressure to outlet static pressure
          (ft-lb)/(sec)

R_a gas constant for air, 53.35 (ft-lb)/(lb-°F)

R_b gas constant for combustion products (ft-lb)/(lb-°F)

Re   Reynolds number

T gas temperature (°F absolute)

T_1 total temperature at nozzle-box inlet (°F absolute)

u blade pitch-line speed (fps)

v theoretical jet speed (fps)

v_a average axial component of turbine discharge velocity (fps)

γ ratio of specific heat at constant pressure to specific heat
          at constant volume

η turbine efficiency defined as ratio of shaft power to theoret-
          ical power computed from total temperature and pressure at
          turbine inlet and static pressure at the turbine discharge

η_s value of η at standard value of $p_1/T_1^{1.1}$
          $\left(0.009 \text{ in. Hg}/(\text{°F absolute})^{1.1}\right)$

η' turbine efficiency defined as ratio of shaft power to dif-
          ference between theoretical power and kinetic power corre-
          sponding to average axial component of velocity at tur-
          bine discharge

μ viscosity of combustion products (lb-sec)/(sq ft)

METHOD OF ANALYSIS

The turbine efficiency for the tests reported herein was calculated according to the methods of references 2 and 3. The calculations of air flow were made according to the standard practice of the A.S.M.E.

The efficiency of a gas turbine of the constant-pressure type is assumed to be a function of the blade-to-jet speed ratio, the pressure ratio, and the Reynolds number. Other variables, such as leakage, windage, heat losses, and bearing friction, are assumed to be of secondary importance or dependent on the principal variables. This statement may be written in the following equation:

$$\eta = f(u/v, \ p_1/p_d, \ Re) \tag{1}$$

If the assumption is made that viscosity is proportional to T^n, where n is a constant, the theoretical Reynolds number corresponding to the theoretical jet velocity v is given by

$$Re = \frac{\rho v L}{\mu} = \frac{L p_1 (70.73)}{K_1 T_1^{\ n} \ R_b T_1} \left(\frac{p_d}{p_1}\right)^{\frac{1+n-n\gamma}{\gamma}} \sqrt{2g \ \frac{\gamma}{\gamma-1} \ R_b T_1 \left[1 - \left(\frac{p_d}{p_1}\right)^{\frac{\gamma-1}{\gamma}}\right]} \tag{2}$$

where K_1 is a constant depending on the viscosity of the fluid, ρ is the theoretical density corresponding to the theoretical jet velocity, and L is a characteristic dimension of the turbine. For a given turbine, L is constant. If the variations of γ and R_b are neglected, the Reynolds number (equation (2)) for a given turbine and fluid becomes

$$Re = \frac{p_1}{T_1^{\left(n + \frac{1}{2}\right)}} \ f\left(\frac{p_1}{p_d}\right) \tag{3}$$

Inasmuch as the ratio p_1/p_d is already listed as a variable in equation (1), the only new variable added by the Reynolds number is the ratio of $p_1/T_1^{\left(n + \frac{1}{2}\right)}$. Equation (1) may then be written

$$\eta = f\left[u/v, \ p_1/p_d, \ p_1/T_1^{\left(n + \frac{1}{2}\right)}\right] \tag{4}$$

Although the Reynolds number corresponding to isentropic flow was used to establish the factor $p_1/T_1^{\left(n + \frac{1}{2}\right)}$, the Reynolds number of the flow over the buckets change only by functions of p_1/p_d and u/v and thus introduce no new variables.

A logarithmic plot (fig. 5) of viscosity of air against the absolute temperature reveals that for the range of temperatures from 1000° to 2000° F absolute there is very little variation from a straight line with a slope of approximately 0.6. The slope of the curve for lower temperatures is slightly greater. The data for this curve were taken from reference 4. The composition of the working fluid during the tests varied negligibly from that of air. Equation (4) then reduces to:

$$\eta = f\left(u/v, \quad p_1/p_d, \quad p_1/T_1^{1.1}\right) \tag{5}$$

The variables for correlating the mass-flow data of the turbine are revealed by a consideration of the equation for mass flow through either an ideal or a convergent nozzle; both show the same variables. The mass flow through an ideal nozzle of area A for example, is given by

$$M_t = \rho A v = \frac{p_1(70.73)}{gR_bT_1}\left(\frac{p_d}{p_1}\right)^{\frac{1}{\gamma}} A \sqrt{2g\frac{\gamma}{\gamma-1}R_bT_1\left[1 - \left(\frac{p_d}{p_1}\right)^{\frac{\gamma-1}{\gamma}}\right]} \tag{6}$$

where ρ is the theoretical density at the nozzle exit and v is the theoretical velocity at the nozzle exit. This relation reveals that the quantity $\frac{M_t}{p_1}\sqrt{gR_bT_1}$ is a function of p_d/p_1. The equation for mass flow through a simple converging nozzle in the supersonic range indicates that in this range $\frac{M_t}{p_1}\sqrt{gR_bT_1}$ is a constant. The presence of the turbine wheel introduces some interference with the flow from the nozzle. It is reasonable to expect that the amount of interference depends on the blade-to-jet speed ratio. The theoretical jet speed is given by

$$v = \sqrt{2\frac{\gamma}{\gamma-1}gR_bT_1\left[1 - \left(\frac{p_d}{p_1}\right)^{\frac{\gamma-1}{\gamma}}\right]} \tag{7}$$

The blade speed u for a given turbine is proportional to the turbine speed N. The ratio u/v is therefore proportional to $\sqrt{519/T_1}$ N f(p_1/p_d). The ratio p_1/p_d has already been listed as one of the variables for plotting the mass-flow factor; thus, the only additional variable indicated by this discussion is $\sqrt{519/T_1}$ N. The tentative correlation of the mass-flow data can be made by plotting the factor $\dfrac{M_t}{p_1} \sqrt{gR_bT_1}$ against p_1/p_d with $\sqrt{519/T_1}$ N as a parameter.

RESULTS

Figures 6 to 8 are conventional curves of the turbine efficiency η plotted against the blade-to-jet speed ratio. They show the effect of the nozzle-box inlet pressure and temperature and the pressure ratio on the turbine efficiency. These curves are all substantially parabolic with maximum efficiency occurring at a blade-to-jet speed ratio of approximately 0.4. The efficiency for a normal operating condition of the turbine in a turbosupercharger (inlet pressure, approximately 27 in. Hg absolute; inlet temperature, 1800° F absolute; blade-to-jet speed ratio, 0.4; and pressure ratio, 2.2) is 59 percent.

Cross plots showing the variation of turbine efficiency at a constant blade-to-jet speed ratio (0.4) with the three variables are presented in figure 9. The general trend of the efficiency variation is more easily visualized from these curves than from those in figures 6 to 8. Figure 9(a) shows that maximum efficiency occurs at a pressure ratio of approximately 3 and figure 9(b) shows that efficiency decreases as nozzle-box inlet temperature increases. The increase in efficiency with nozzle-box inlet pressure is presented in figure 9(c). Plots of the curves of figures 9(b) and 9(c) on logarithmic paper indicate that the efficiency varies with the inlet temperature to the -0.075 power and with the inlet pressure to the 0.067 power over the range of tests. The ratio of these exponents is 1.12.

It has been shown in the method of analysis that, for constant pressure ratios and blade-to-jet speed ratios, the turbine efficiency is a function of the ratio of nozzle-box inlet pressure to the 1.1 power of the inlet temperature. Plots of the turbine efficiency against the factor $p_1/T_1^{1.1}$ are shown in figure 10. Curves are shown for variable pressure ratio at several constant blade-to-jet speed ratios. Very good correlation is noted in the data for the inlet-temperature range shown (1200° to 2000° F absolute) and for inlet pressures from 10 to 60 inches of mercury absolute. The set of points corresponding to the air tests with an inlet temperature

of 550° F absolute are slightly displaced from the faired curves;
the magnitude of the displacement does not exceed $2\frac{1}{2}$ percent in
efficiency (fig. 10). This displacement may be caused by the changing
slope of the viscosity curve at temperatures less than 1000° F abso-
lute. The good correlation obtained with the factor $p_1/T_1{}^{1.1}$ indi-
cates that the change of turbine efficiency with nozzle-box inlet
temperature and pressure for constant pressure ratio and blade-to-jet
speed ratio may be a Reynolds number effect. Further investigation
is required, however, to establish this fact conclusively because of
the small changes in efficiency involved.

The parallelism of the curves of constant pressure ratio at a
given value of blade-to-jet speed ratio u/v in figure 10 suggested
the following procedure for condensing the presentation of the tur-
bine efficiency: For any given pressure ratio the quantity η_s is
defined as the value of the turbine efficiency at a value of
$p_1/T_1{}^{1.1}$ of 0.009 inch mercury per (°F absolute)$^{1.1}$. These values
of η_s are shown in figure 11(a) plotted against u/v for various
values of p_1/p_d.

The values of turbine efficiency for other than the standard
value of $p_1/T_1{}^{1.1}$ are divided by the value of η_s for the same
value of u/v and p_1/p_d and are plotted against $p_1/T_1{}^{1.1}$ for
various values of u/v in figure 11(b). For a given value of u/v
and $p_1/T_1{}^{1.1}$ the value of η/η_s is nearly independent of p_1/p_d.
This sort of plot is an expedient that works fairly well in the
present case but cannot be generally recommended. The more accurate
and fundamentally more sound presentation is that of figure 10. In
other types of turbine, the correlation of figure 10 may not hold
inasmuch as there is no assurance that Reynolds number will affect
a turbine of different design in the same manner or that other fac-
tors not involving the Reynolds number will not cause some variation.

The accuracy of the correlation varies somewhat with the oper-
ating conditions. Figure 12 shows an example of a curve calculated
from figure 11 and an experimental curve. The slight scatter shown
is typical of the maximum variation to be expected, approximately
±1 percent in efficiency, over the temperature range from 1200° to
2000° F absolute. The data at 550° F absolute show a somewhat
larger scatter; the maximum scatter of approximately $2\frac{1}{2}$ percent in
efficiency occurred at pressure ratios less than 2.

Figure 13 is a plot of the gas-flow factor $\frac{M_t}{p_1}\sqrt{gR_bT_1}$ against
the pressure ratio and the product of the turbine speed and the
square root of the ratio of NACA standard sea-level temperature to
the nozzle-box inlet temperature. This ratio is proportional to
the blade-to-jet speed ratio for a constant pressure ratio. From
figure 13(a), the gas flow can be correlated within ±1.5 percent
for the range of test values of p_1 and for a range of T_1 from
1200° to 2000° F absolute. Because the data for an inlet tempera-
ture of 550° F absolute did not fall on the same curve, an addi-
tional chart (fig. 13(b)) is shown for these data. Cross plots of
figures 13(a) and 13(b) are shown in figures 13(c) and 13(d). With
figures 11 and 13, and reference 3, the turbine power for any condi-
tion covered by the reported tests may be calculated.

The results of tests with the nozzle box insulated are compared
with tests in which the nozzle box was not insulated in figure 14.
No air was blown over the nozzle box in the uninsulated tests. It
is evident from figure 14 that the difference in performance caused
by the insulation was small and within the magnitude of experimental
error. Although the curves are given only for a pressure ratio of
2.2, data on other pressure ratios show similar results. It may be
concluded that, for inlet-gas temperatures from 1200° to 1800° F
absolute, the differences in efficiency for the cases of insulated
and uninsulated nozzle box are negligible when the air external to
the nozzle box is quiet.

The turbine efficiency as previously defined gives the shaft
work as a ratio of the theoretical work for an expansion from the
total pressure at the turbine inlet to the static pressure at the
turbine outlet. This efficiency includes in the theoretical power
available some energy that may be utilized for jet propulsion or
in succeeding turbine stages. In applications where the turbine-
discharge velocity is utilized for jet propulsion, it is appro-
priate to define an efficiency in which the turbine is credited for
the kinetic energy of the discharge jet. A number of definitions
of this efficiency are possible. In the choice of a definition,
consideration should be given to the ease of measurement and compu-
tation and to the practical aspect of the portion of the discharge
velocity recoverable for jet propulsion. In the present report the
turbine efficiency under discussion is defined as

$$\eta' = \frac{P_t}{P_{th} - \frac{1}{2}M_t v_a^2} \tag{8}$$

The value of v_a is equal to the mass flow of gas divided by the
bucket annular area A_d and the gas density at the bucket exit and

is given by the equation

$$v_a = \sqrt{\left(\frac{\gamma}{\gamma-1} \, 70.73 \, \frac{P_d A_d}{M_t}\right)^2 + \left(2g \, \frac{\gamma}{\gamma-1} \, R_b T_1 - \frac{2P_t}{M_t}\right)} - \frac{\gamma}{\gamma-1} \, 70.73 \frac{P_d A_d}{M_t} \quad (9)$$

It is apparent that the turbine is credited in equation (8) with the kinetic energy corresponding to the energy of the axial component of this average discharge velocity. Theoretically, the total discharge velocity can possibly be utilized for jet propulsion by means of properly shaped guide vanes. Because of the changing angle of attack at the guide vanes with changing operating conditions a set of vanes that may be good for one condition may be poor at others; furthermore, because the total velocity varies with radial and angular position, a survey would be required for its determination. The average axial velocity v_a, on the other hand, can be computed from the measured mass flow of gas and the area swept by the buckets. It is evident that the proposed definition of turbine efficiency is not without objection but it does have the advantage that it may be readily calculated.

Figure 15 shows a plot of η'/η where η' was calculated by the turbine-efficiency equation (8). The values of η' range from about 5 to 22 percent higher than the corresponding values of η; the ratio η'/η is higher for higher pressure ratios and lower blade-to-jet speed ratios. All the data over the range of temperatures from 1200° to 2000° F absolute and inlet pressures from 10.3 to 59.7 inches of mercury absolute are correlated on this curve with an accuracy of ±1 percent. For any given value of pressure ratio and blade-to-jet speed ratio the quantity η'/η is seen to be independent of inlet temperature and pressure. From figures 11 and 15, the efficiency η' may be calculated for any condition within this range.

SUMMARY OF RESULTS

Efficiency tests on a single-stage impulse turbine having an 11.0-inch pitch-line diameter wheel with inserted buckets and a fabricated nozzle diaphragm over a range of inlet pressures from 10 to 60 inches of mercury absolute and inlet temperatures from 1000° to 2000° F absolute have indicated the following results:

1. The efficiency for a normal operating condition (inlet pressure, approximately 27 in. Hg absolute; inlet temperature, 1800° F absolute; blade-to-jet speed ratio, 0.4; and pressure ratio, 2.2) was 59 percent.

2. The change in turbine efficiency for constant pressure ratio and blade-to-jet speed ratio over a range of inlet temperatures and pressures was correlated against the factor $p_1/T_1^{1.1}$, which was derived from the Reynolds number equation

where

p_1 total inlet pressure (in. Hg absolute)

T_1 total inlet temperature ($^\circ$F absolute)

This result indicates that the variation in turbine efficiency with inlet conditions for a constant pressure ratio and blade-to-jet speed ratio may be principally a Reynolds number effect.

3. The air flow could be correlated with an accuracy of ± 1.5 percent over the range of inlet temperatures from 1200° to 2000° F absolute and total inlet pressures from 10 to 60 inches of mercury absolute by plotting $\dfrac{M_t}{p_1}\sqrt{gR_bT_1}$ against the pressure ratio and blade-to-jet speed ratio

where

M_t mass flow of air plus fuel (slugs)/(sec)

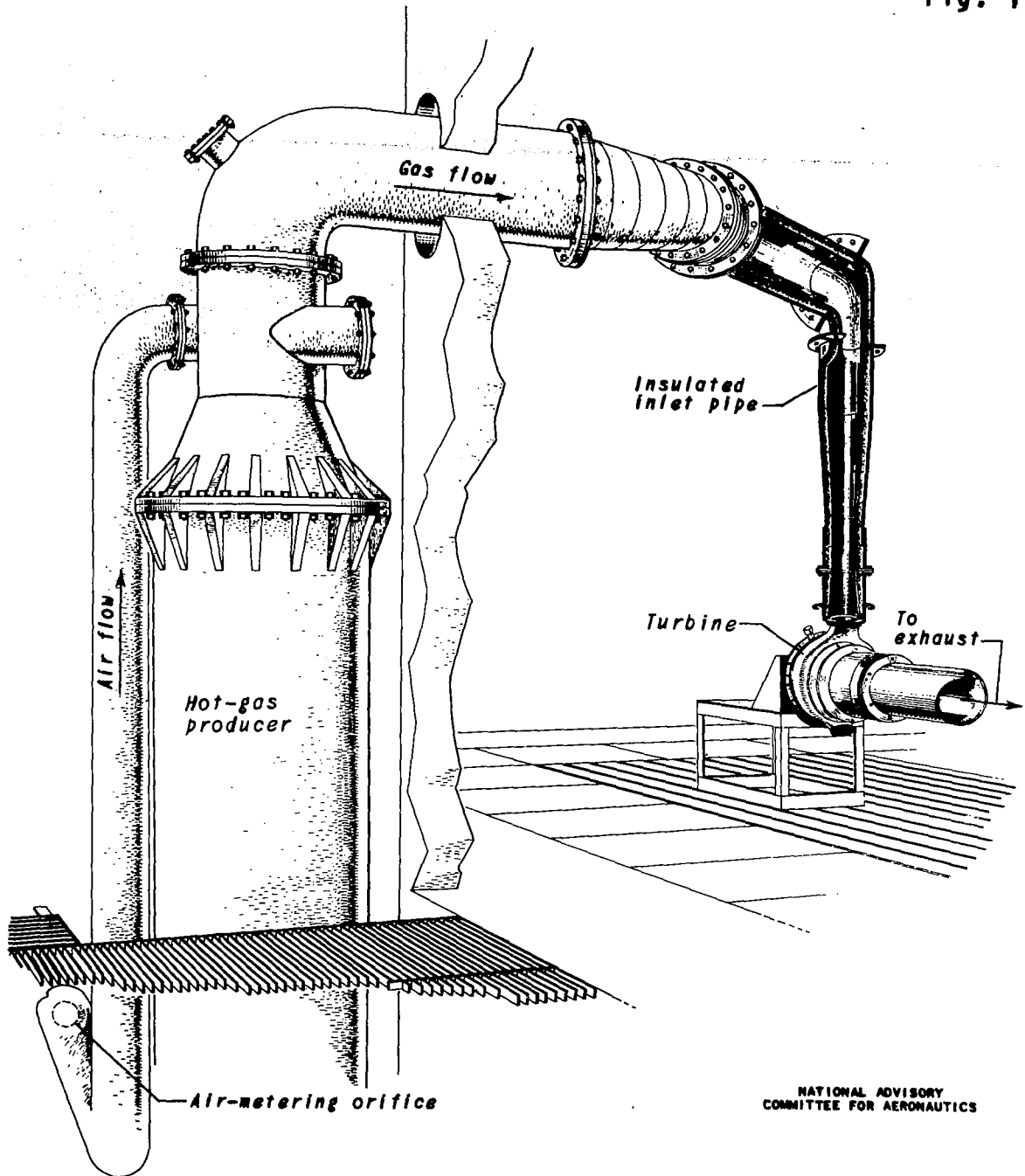R_b gas constant for combustion products (ft-lb)/(lb-$^\circ$F)

4. Over the range of inlet gas temperatures from 1200° to 1800° F absolute, insulating the nozzle box caused no change in the turbine efficiency, as compared with tests of an uninsulated nozzle box in which the external air was quiet.

5. In the computation of turbine efficiency when the turbine is credited with the kinetic energy corresponding to the average axial component of the velocity behind the turbine buckets, an increase in efficiency between 5 and 22 percent for pressure ratios between 1.4 and 5.2 and blade-to-jet speed ratios between 0.1 and 0.6 was obtained. In general, the larger changes in efficiency occurred at the smaller blade-to-jet speed ratios and the larger pressure ratios.

Aircraft Engine Research Laboratory,
    National Advisory Committee for Aeronautics,
        Cleveland, Ohio.

REFERENCES

1. Moore, Charles S., Biermann, Arnold E., and Voss, Fred: The
   NACA Balanced-Diaphragm Dynamometer-Torque Indicator. NACA
   RB No. 4C28, 1944.

2. Gabriel, David S., and Carman, L. Robert: Efficiency Tests of
   a Single-Stage Impulse Turbine Having an 11.0-Inch Pitch-Line
   Diameter Wheel with Air as the Driving Fluid. NACA ACR No. E5C30,
   1945.

3. Pinkel, Benjamin, and Turner, L. Richard: Thermodynamic Data
   for the Computation of the Performance of Exhaust-Gas Turbines.
   NACA ARR No. 4B25, 1944.

4. Boelter, L. M. K., and Sharp, W. H.: An Investigation of Aircraft
   Heaters. XVI - Determination of the Viscosity of Exhaust Gases
   from a Gasoline Engine. NACA ARR No. 4F24, 1944.

Figure 1. – Schematic diagram of test setup showing hot-gas producer.

Fig. 2.   NACA ACR No. E5E19
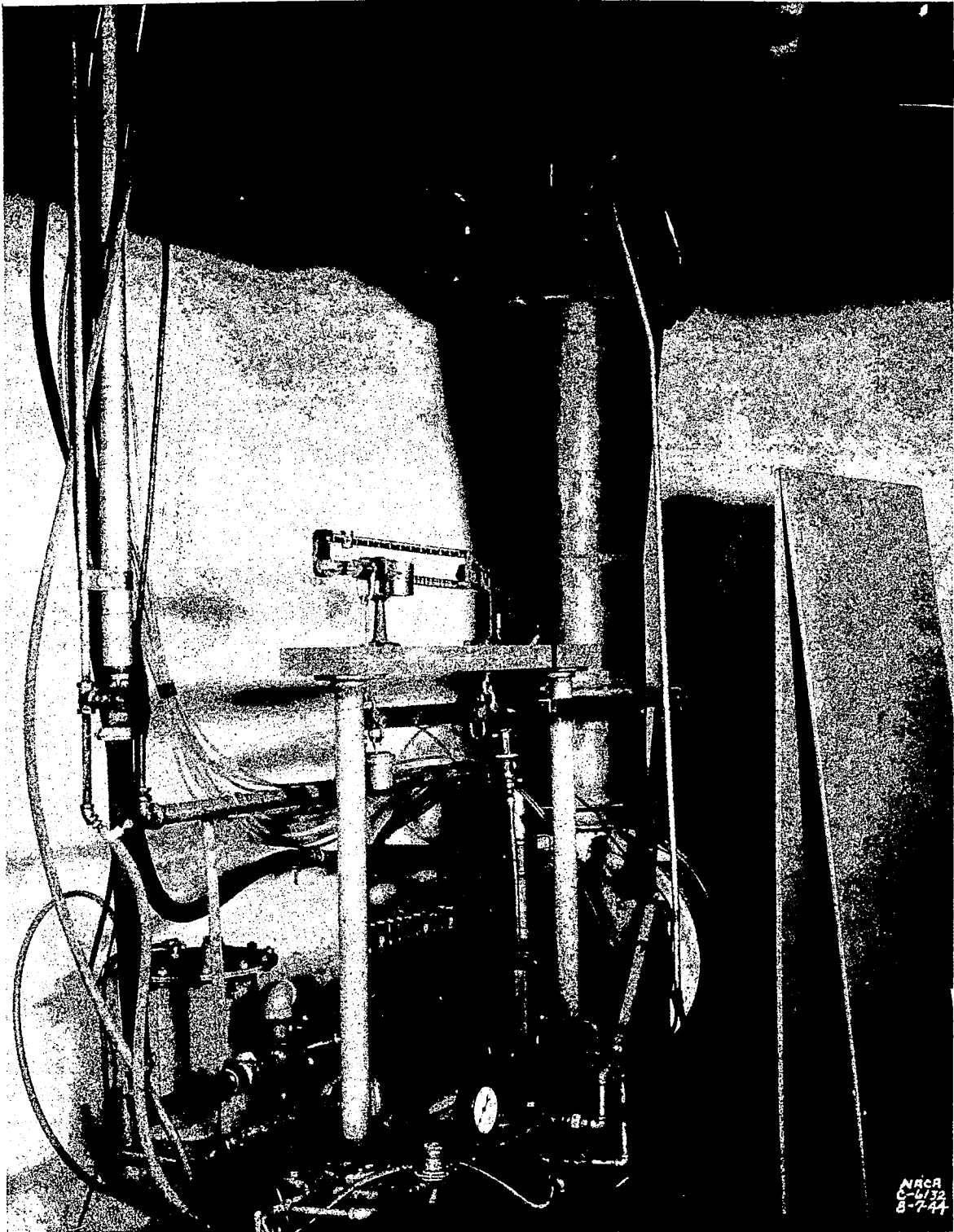
Figure 2. – Photograph of test apparatus showing turbine and dynamometer arrangement.

Inlet
temperature, T_i

Nozzle-box inlet
pressure

Air in

To exhaust

Detail at A

Jet pump

Nozzle-box
baffle

Dynamometer shaft

To exhaust

Plugs

Pressure-
balancing
chamber

See detail A

Discharge
pressure, p_d

Labyrinth
seal gland

Cooling caps

Housing

Figure 3. - Schematic diagram showing the turbine housing
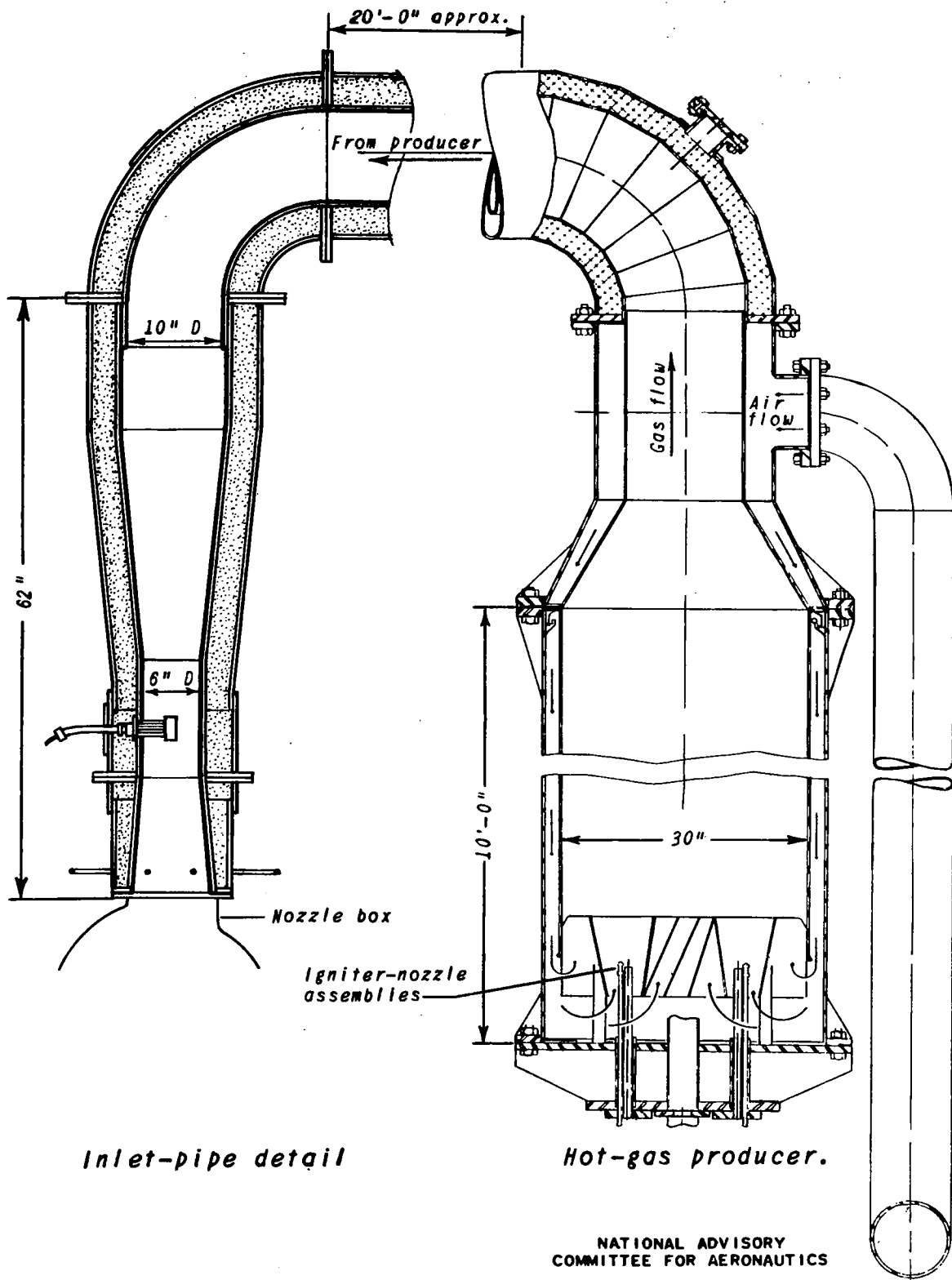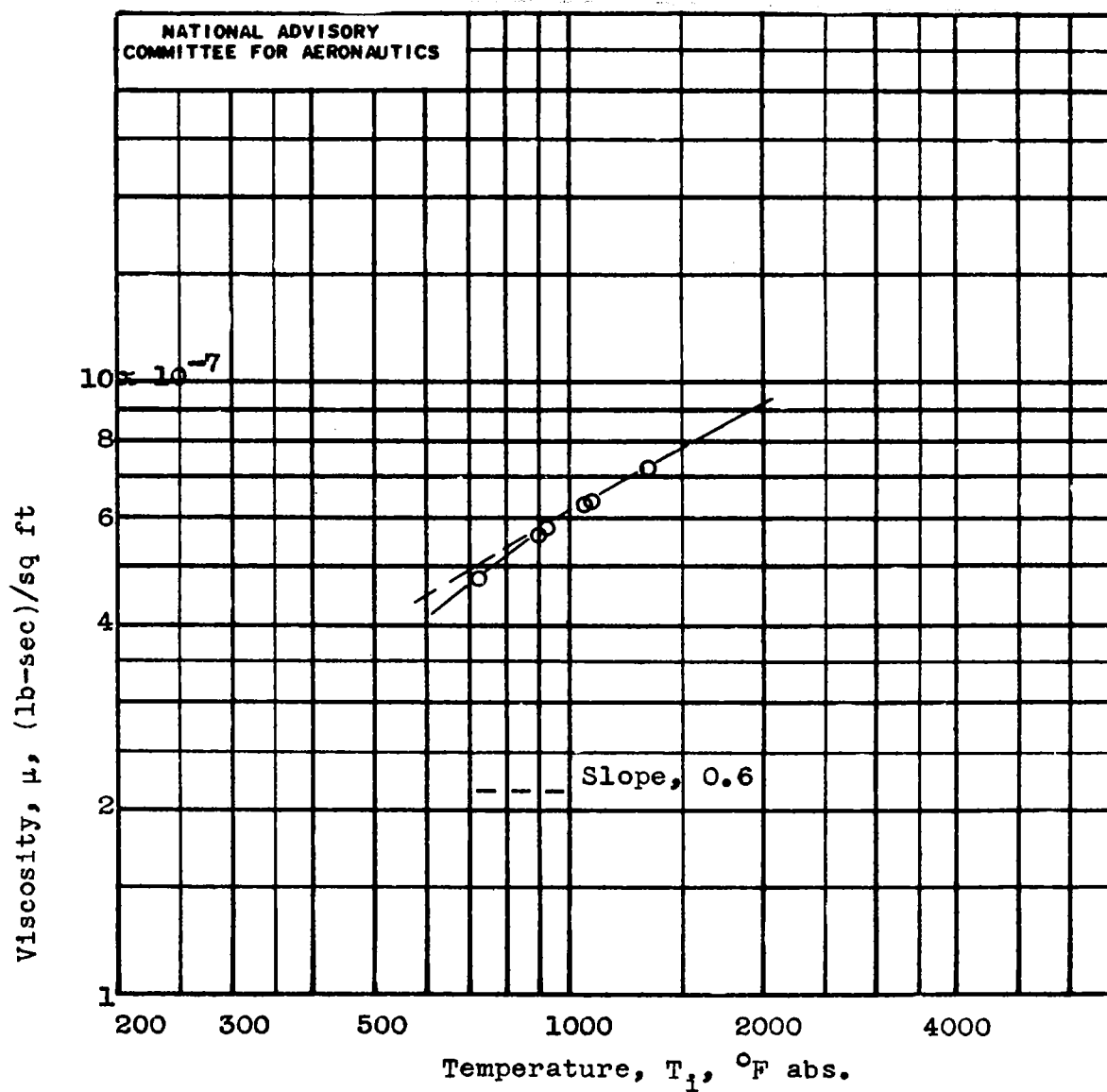 and the location of the various points where measurements
  were made.

Fig. 4   NACA ACR No. E5E19

20'-0" approx.

From producer

10" D

62"

6" D

Gas flow

Air flow

30"

10'-0"

Nozzle box

Igniter-nozzle assemblies

Inlet-pipe detail   Hot-gas producer.

NATIONAL ADVISORY
COMMITTEE FOR AERONAUTICS

Figure 4. - Inlet system.

Figure 5.— Variation of the viscosity of air with temperature.

Fig. 6   NACA ACR No. E5E19

(a) Inlet temperature, 550° F absolute.

(b) Inlet temperature, 1200° F absolute.

(c) Inlet temperature, 1800° F absolute.
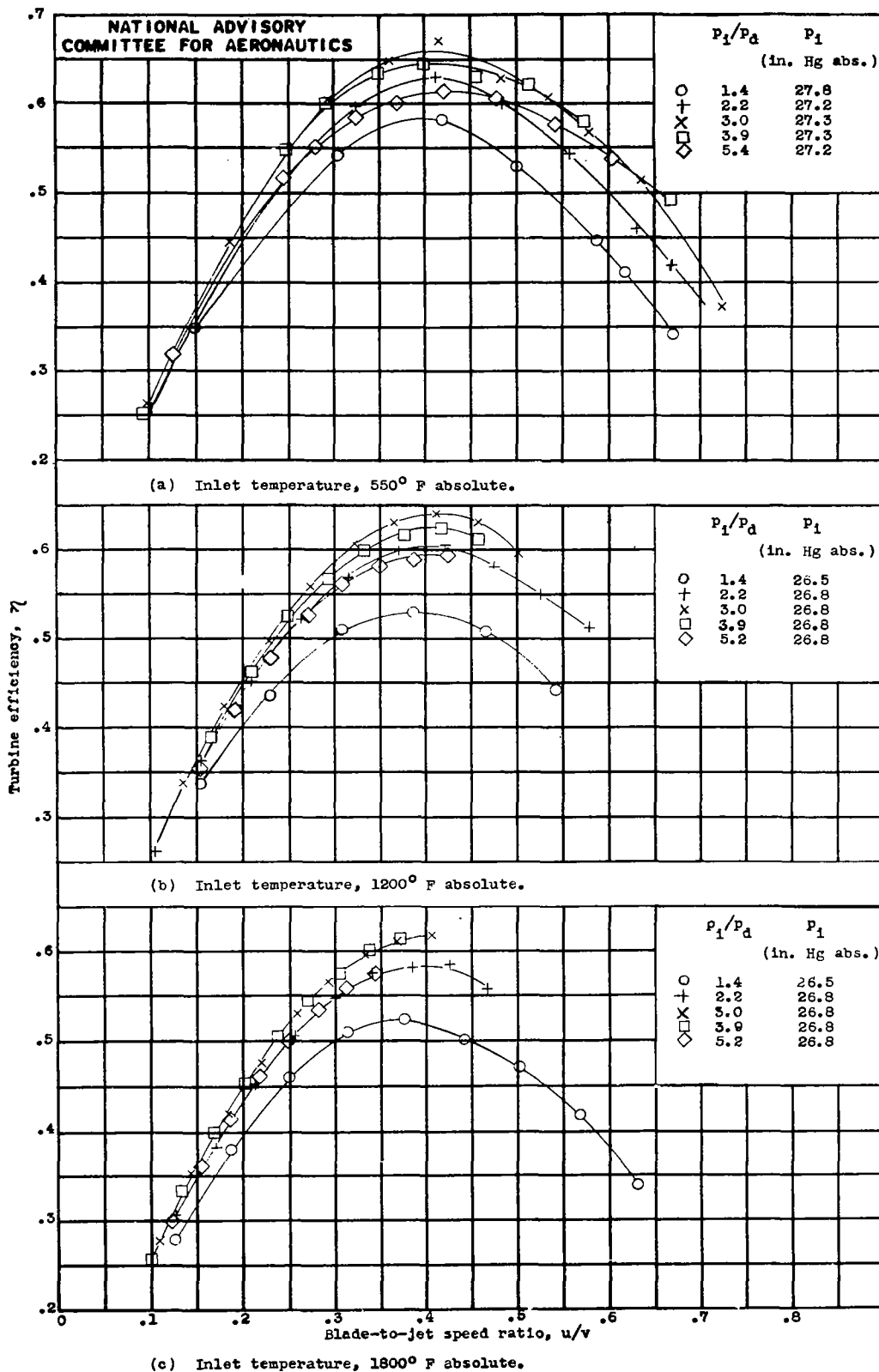
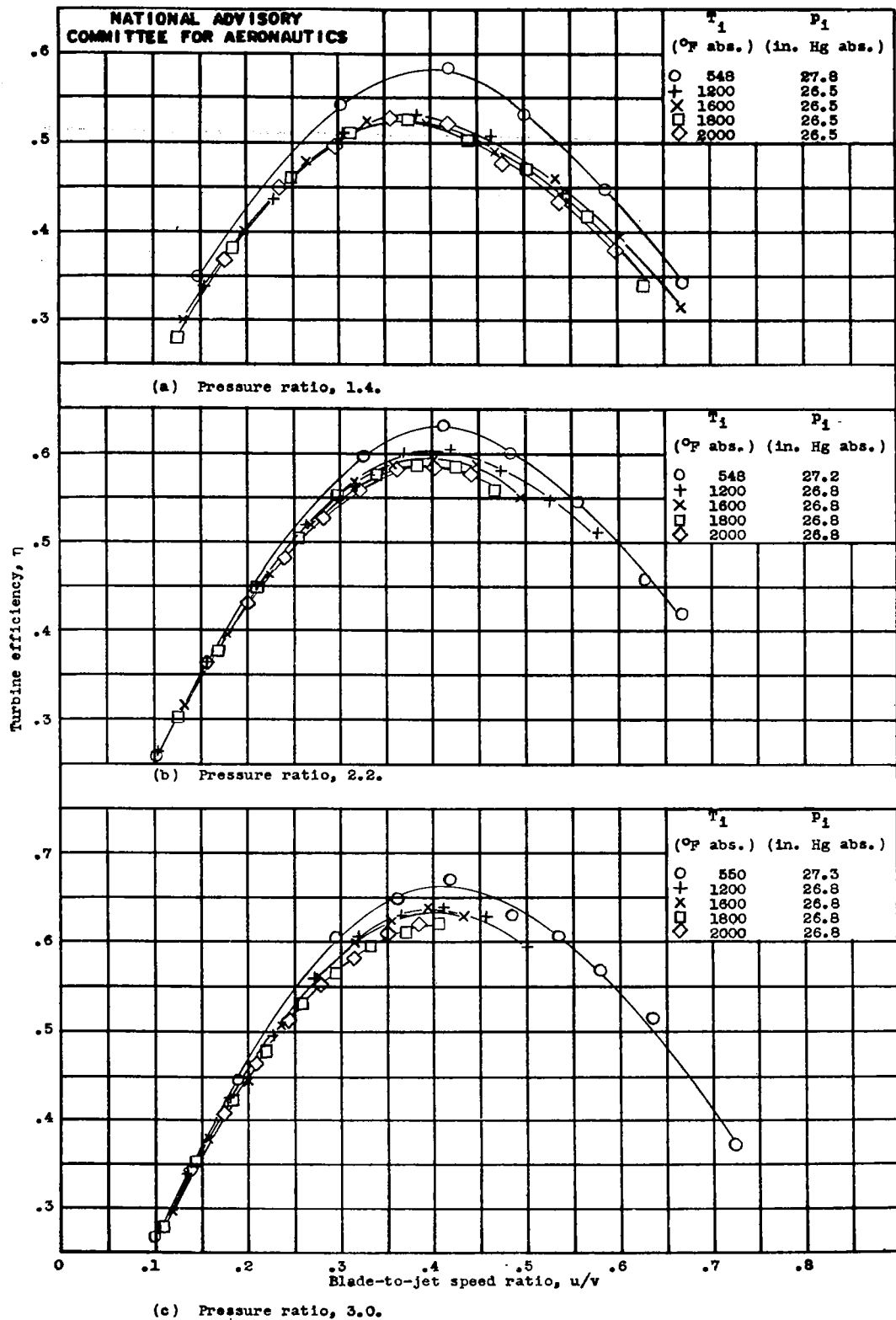Figure 6.- Variation of turbine efficiency with blade-to-jet speed ratio for various pressure ratios.

(a) Pressure ratio, 1.4.

(b) Pressure ratio, 2.2.

(c) Pressure ratio, 3.0.

Figure 7.- Variation of turbine efficiency with blade-to-jet speed ratio for various inlet temperatures.
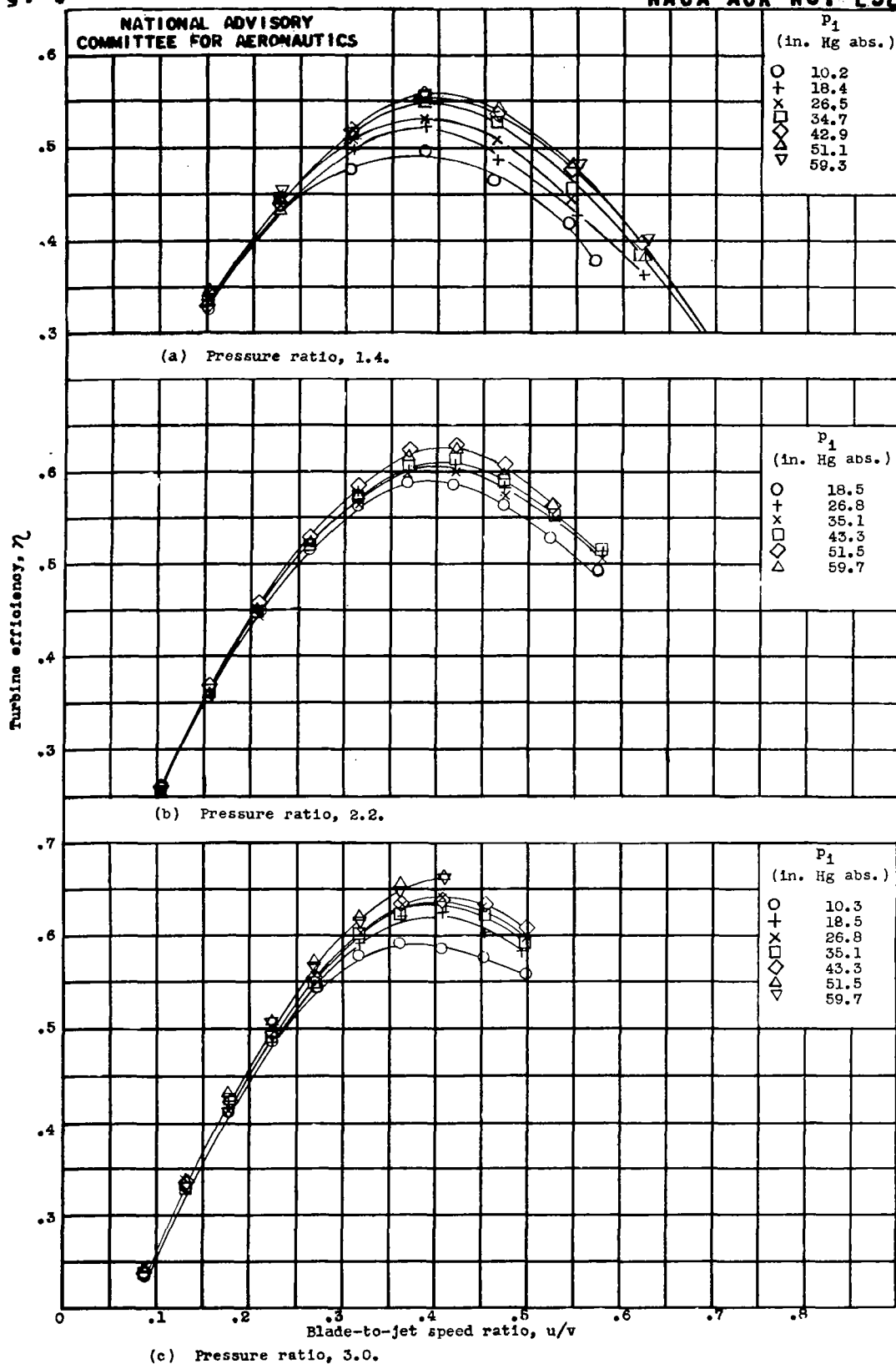
Fig. 8

NACA ACR No. E5E19

(a) Pressure ratio, 1.4.

(b) Pressure ratio, 2.2.

(c) Pressure ratio, 3.0.

Figure 8.— Variation of turbine efficiency with blade-to-jet speed ratio for various inlet pressures. Inlet temperature, 1200° F absolute.

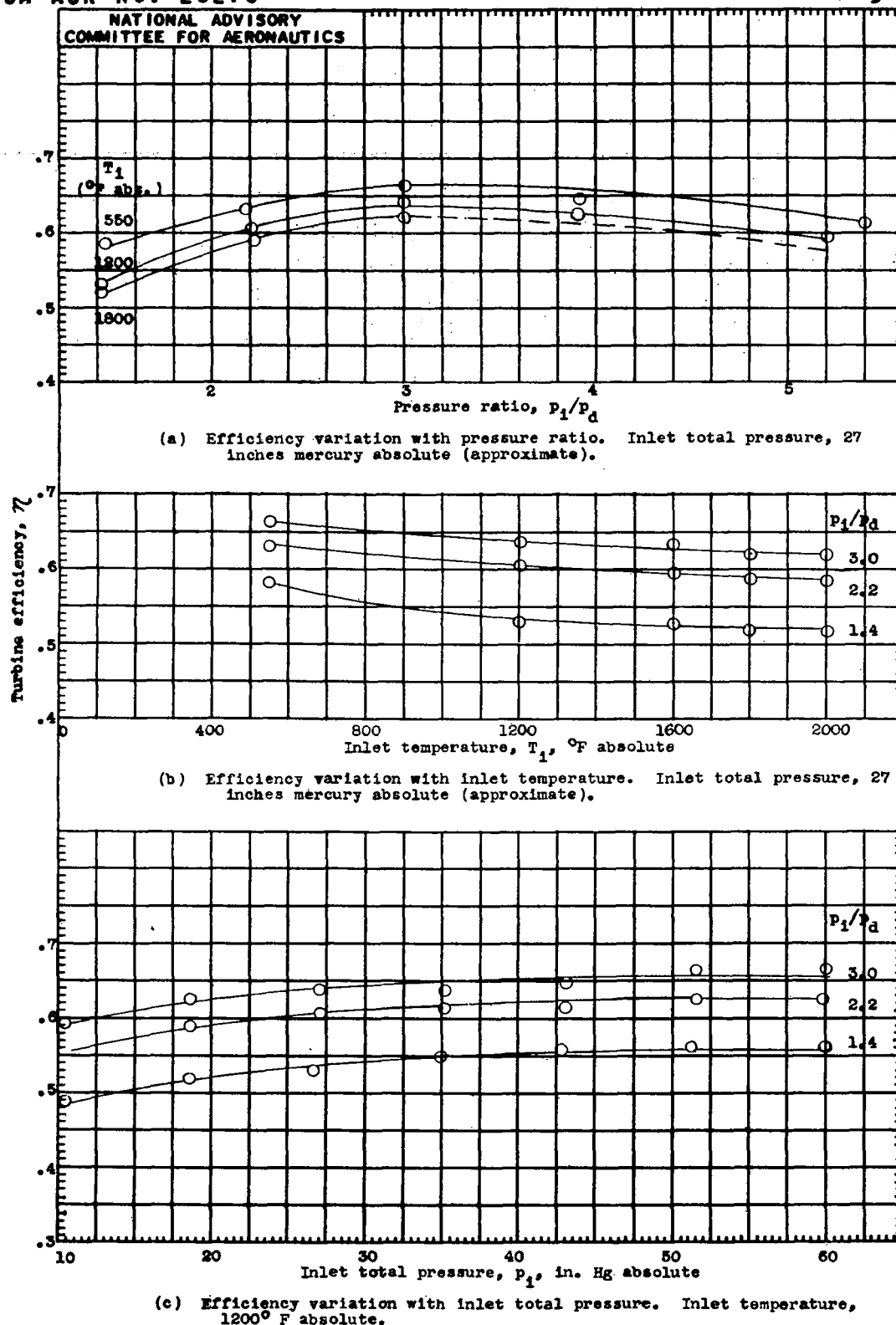NATIONAL ADVISORY
COMMITTEE FOR AERONAUTICS

(a) Efficiency variation with pressure ratio. Inlet total pressure, 27
     inches mercury absolute (approximate).

(b) Efficiency variation with inlet temperature. Inlet total pressure, 27
     inches mercury absolute (approximate).

(c) Efficiency variation with inlet total pressure. Inlet temperature,
     1200° F absolute.

Figure 9.- Variation of turbine efficiency with pressure ratio, inlet temperature, and
inlet total pressure. Blade-to-jet speed ratio, 0.4.

Fig. 10   NACA ACR No. E5E19

Figure 10.- Variation of turbine efficiency with Reynolds number factor.

(a) Variation of efficiency standard with blade-to-jet speed ratio; $p_1/T_1^{1.1}$, 0.009.

(b) Variation of the efficiency ratio with the Reynolds number factor.

Figure 11.— Turbine—efficiency correlation.

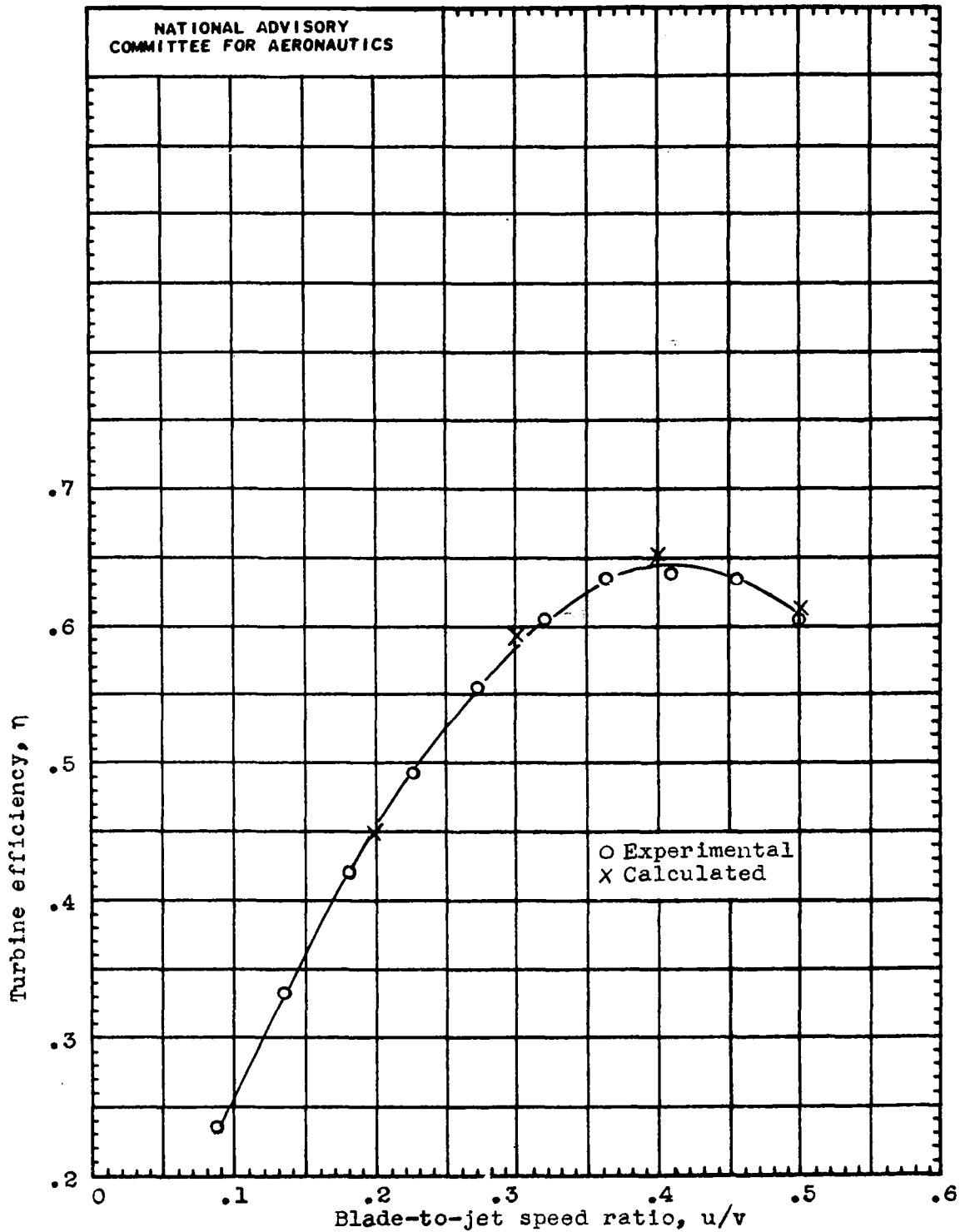Fig. 12   NACA ACR No. E5E19

Figure 12.— Comparison between calculated and experimental data. Inlet total pressure, 43.3 inches mercury absolute; inlet temperature, 1200° F absolute; p_i/p_d, 3.0.
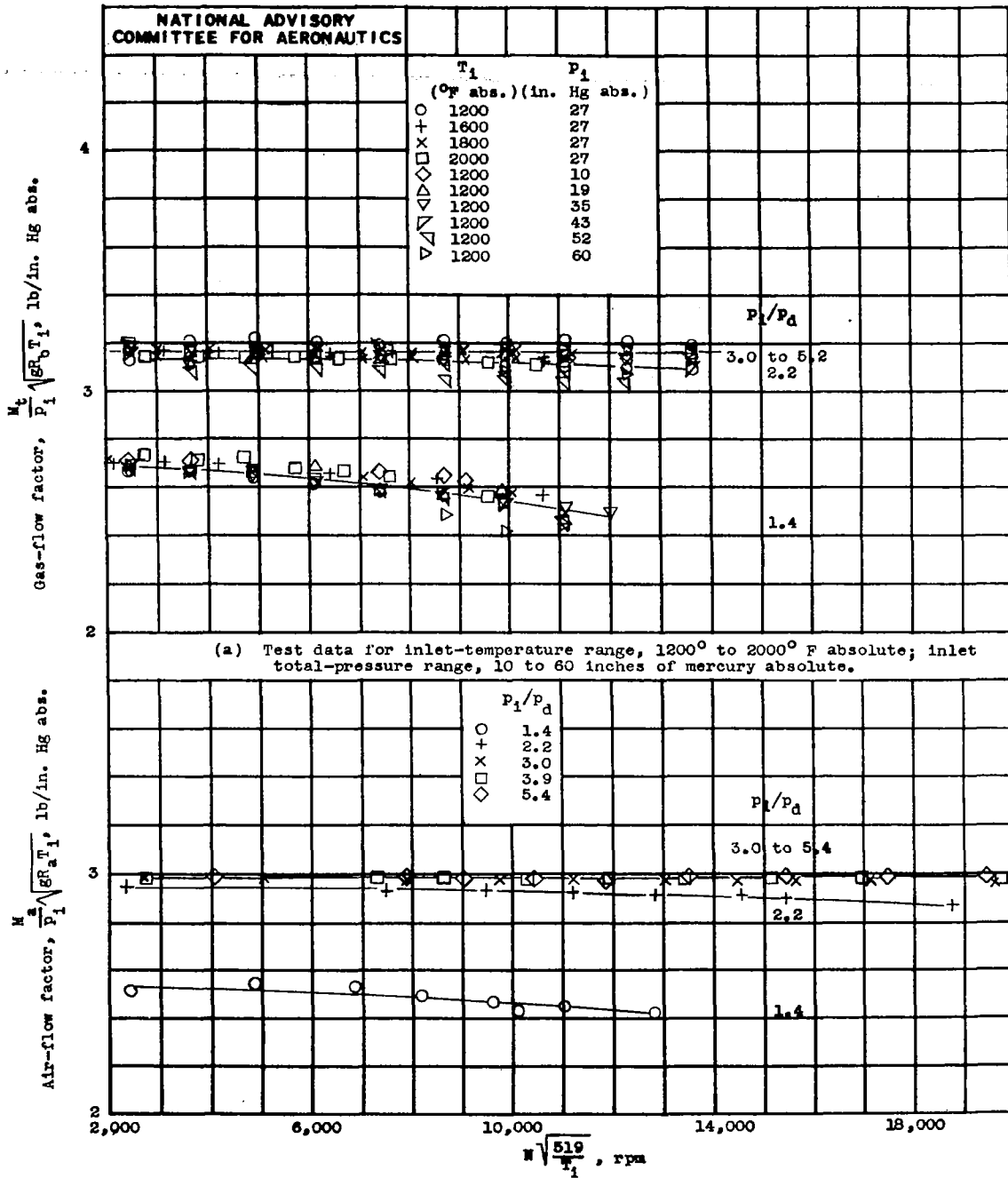
(a) Test data for inlet-temperature range, 1200° to 2000° F absolute; inlet total-pressure range, 10 to 60 inches of mercury absolute.

(b) Test data for inlet temperature, 550° F absolute.

Figure 13.- Correlation of the gas-flow data.

(c) Cross plots for inlet temperature range, 1200° to 2000° F absolute; inlet-pressure range, 10 to 60 inches of mercury absolute.

(d) Cross plots for inlet temperature, 550° F absolute.
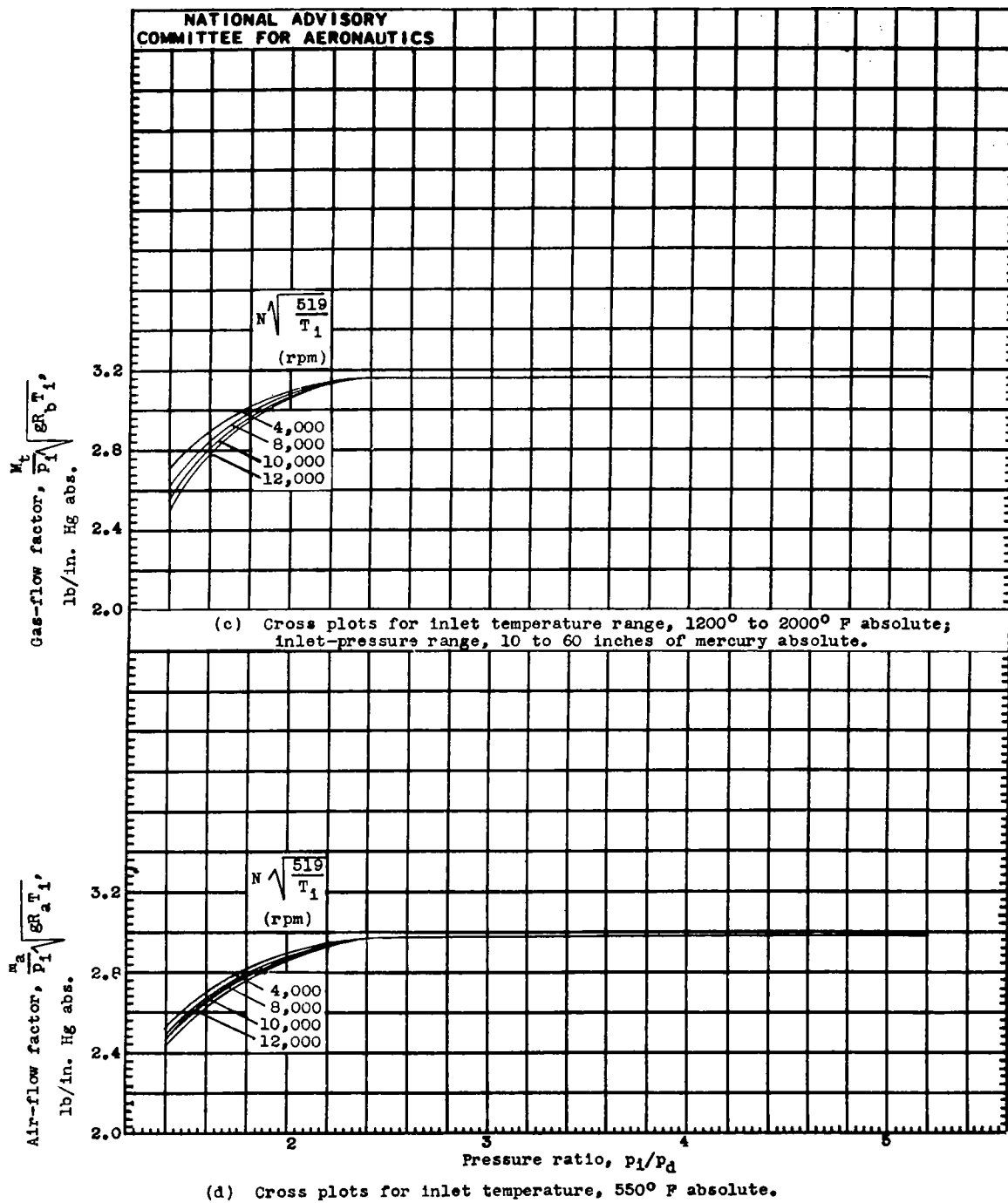
Figure 13. - Concluded. Correlation of the gas-flow data.

NATIONAL ADVISORY
COMMITTEE FOR AERONAUTICS

Nozzle box
O Insulated
+ Uninsulated

(a)   Inlet temperature, 1200° F absolute.

(b)   Inlet temperature, 1600° F absolute.

Turbine efficiency, η

Blade-to-jet speed ratio, u/v

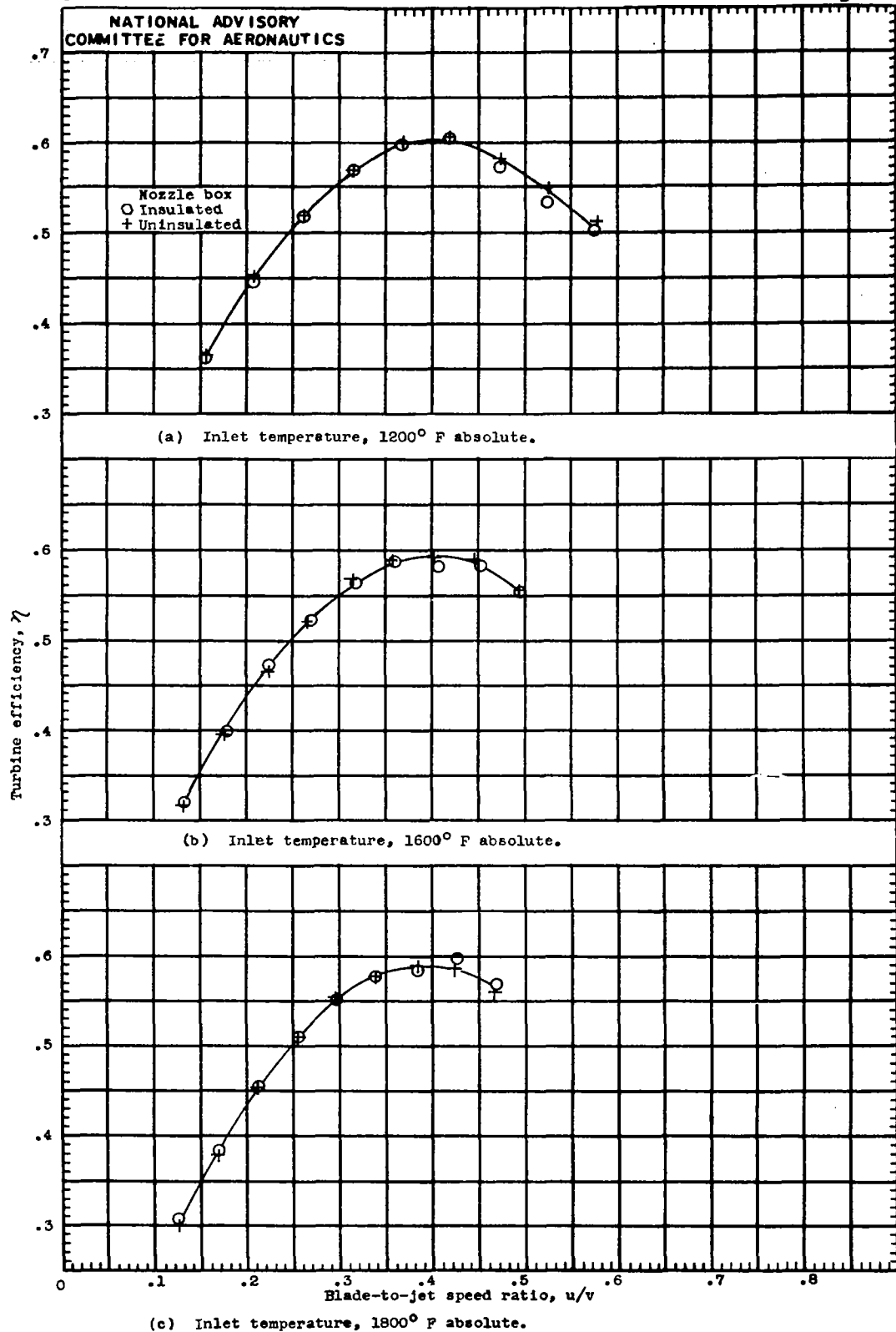(c)   Inlet temperature, 1800° F absolute.

Figure 14.- Comparison of tests using insulated nozzle box with those using uninsulated nozzle
box. Pressure ratio, 2.2; inlet total pressure, 26.8 inches mercury absolute.

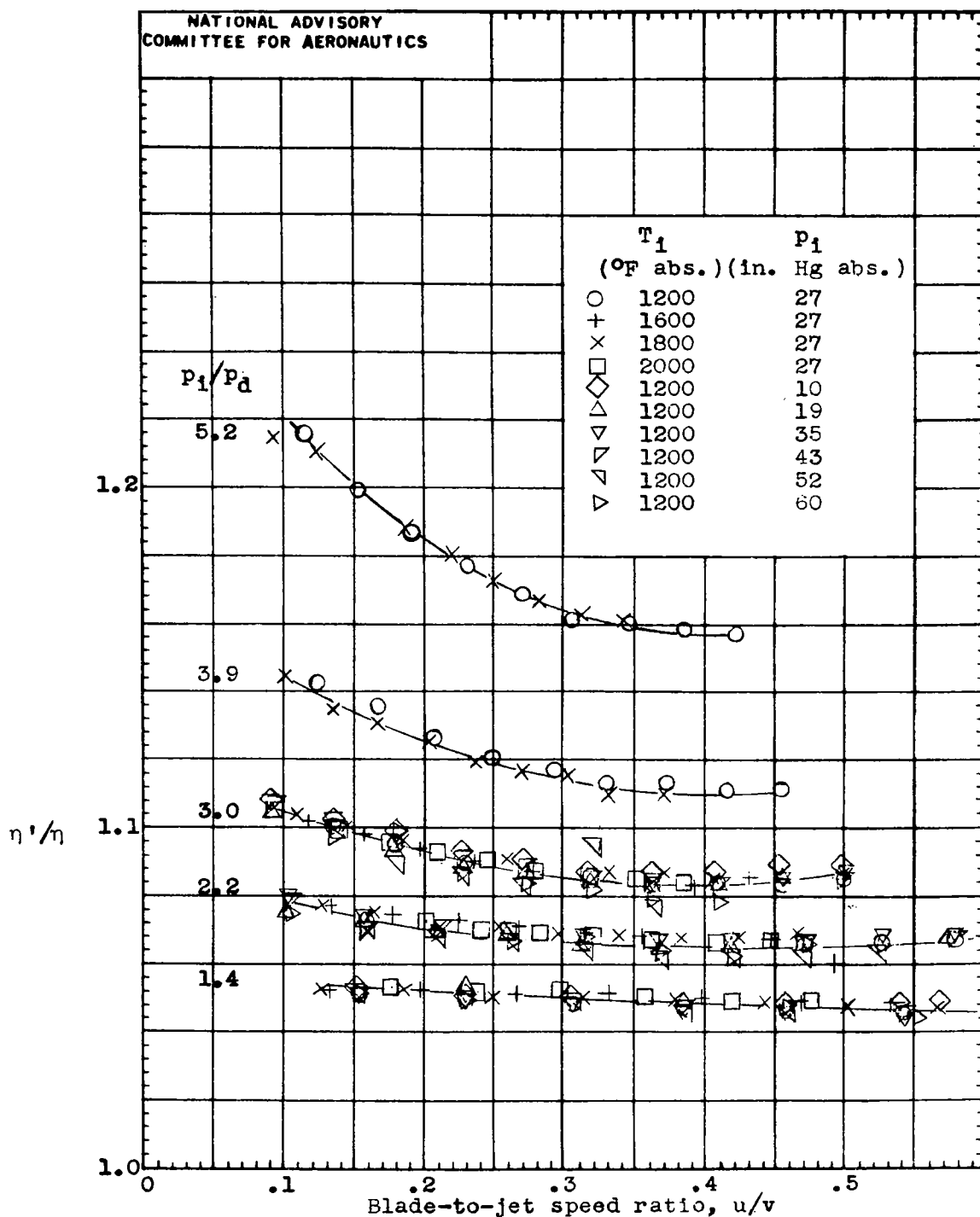Fig. 15   NACA ACR No. E5E19

Figure 15.- Variation of the ratio η'/η with the blade-to-jet speed ratio for various pressure ratios. Inlet-temperature range, 1200° to 2000° F absolute; inlet total-pressure range, 10 to 60 inches of mercury absolute.